RESEARCH ARTICLE OPEN ACCESS

Adaptive Indoor Localization by using Environmental Thresholding and Virtual Fingerprint Technique

Hakan Koyuncu[1], Baki Koyuncu[2]

ABSTRACT
Environmental Thresholding and virtual fingerprinting techniques are deployed with Wireless Sensor Nodes (WSN) to create an adaptive localization system. A virtual fingerprint map of RSSI values is generated across the test area. RSSI amplitude correction phase is introduced with respect to local environmental parameters on virtual and recorded RSSI values at fingerprint grid points and unknown object points. Localization algorithms are employed to determine the unknown object locations. Localization accuracies of around 35cm at a grid space of 1m are obtained during the calculations.
Keywords: WSN, RFID, Adaptive localization, Virtual Fingerprint, threshold, RSSI, k-NN, weighted k-NN

I. INTRODUCTION

Wireless sensor nodes (WSN) are commonly used for object localization in recent years. They are deployed in indoors and outdoors for position detection purposes. Many localization algorithms have been introduced over the years by using received signal strength (RSSI) [1, 2] values. Radio frequency based devices (RFID) are widely used as WSN nodes due to their low cost and low power consumption [3]. Some of the best know localization algorithms are ranged based [4], range free [5], direction of arrival (DOA) [6], Frequency Difference of Arrival (FDA) and Time Difference of Arrival (TDA) algorithms. Additional techniques such as triangulation, trilateration, together with time intervals and RSSI values can be used to find unknown positions.

In literature, an environmentally adaptive path loss localization method is developed by Zhang et al. [7]. In this study, ranging errors are calibrated by broadcasted voltage levels and indoor multi-fading together with antenna effects are used adaptively to generate path lose models. On the other hand, Janire Larranaga et al. has developed another environmentally adaptive localization method [8] where RSSI signal levels are obtained between the communications of WSNs and the environmental effects are taken into account by the signal level changes since the last signal request, [9].

In the current study, a virtual fingerprint map is incorporated into localization calculations [10]. Anchor transmitter WSNs radiate RF signals across the test area. Transmitted signal amplitudes decrease in exponential form against distances in free space [11, 12]. Mathematical formulations of these exponential forms are deployed and virtual RSSI values are theoretically calculated at every grid point. Finally, a virtual fingerprint map is constructed for each anchor transmitter WSN. Virtual RSSI values at grid points are adaptively corrected with respect to environmental factors and the resultant values are deployed in position calculations.

Hence, a new localization technique is proposed in this study where adaptive localization and virtual fingerprint techniques are combined together. After a brief introduction in section 1, theoretical background of adaptive localization and RSSI correction phase is given in section 2. In section 3, virtual fingerprint generation is explained. Results are given in section 4 together with conclusions in section 5.

II. ADAPTIVE LOCALIZATION

WSNs are employed as transmitters and receivers during RSSI measurements. Transmitters are generally placed at the corners of the test area and a receiver is placed on an unknown mobile object as shown in Fig. 1. Received RF signals by the object receiver in RSSI form are sent to a server computer through a wireless media for further processing.

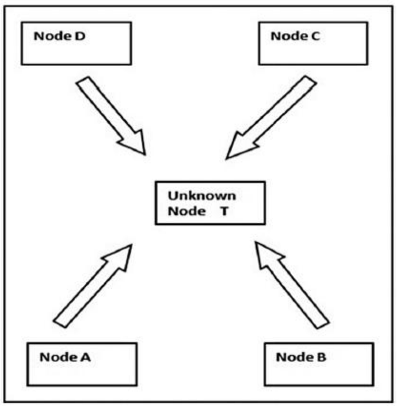

Figure 1: Block diagram of the proposed system across the test area

Environmental factors are identified as the local obstacles and walls around the test areas and the negative effects introduced by them. These obstacles cause multiple reflections of RF signals and the resultant signal additions and cancellations cause random variations in RSSI measurements. RSSI variations must be reduced to minimum values so that accurate localization calculations can be carried out. This reduction is identified as the adaptive correction of RSSI values.

Data frame of N number of RSSI values with an identity code is broadcasted from a transmitter WSN. Object receiver WSN records these RSSI values and sends them to a server computer with respect to specific transmitter. Mean value and the standard deviation of N number of received RSSI values in one frame are defined as R_{Mean} and R_{STD}. To minimize the random behavior of RSSI values, a signal interval of ($R_{Mean} – R_{STD} < R_{Mean} < R_{Mean} + R_{STD}$) is selected and RSSI measurement values only within this interval are considered for localizations.

If there are ‘q’ number of RSSI values in $R_{Mean} \pm R_{STD}$ interval, ‘m’ is taken as the number of RSSI values which are less than or equal to the mean of ‘q’ number of RSSI values. The average value of ‘m’ number of RSSI values is given as

$$R_X = \frac{1}{m}\sum_{i=1}^{m}(RSSI)_i \quad \text{where} \quad (RSSI)_i \le \frac{1}{q}\sum_{J=1}^{q}(RSSI)_J \tag{1}$$

(q–m) is the number of RSSI values whose values are more than the mean of q RSSI values. The average value of (q–m) number of RSSI values is given as

$$R_Y = \frac{1}{q-m}\sum_{i=1}^{q-m}(RSSI)_i \quad \text{where} \quad (RSSI)_i > \frac{1}{q}\sum_{J=1}^{q}(RSSI)_J \tag{2}$$

Hence, RSSI value generated at a measurement location with respect to, transmitter A is expressed as

$$RSSI_A = \beta_A R_X + (1-\beta_A)R_Y \tag{3}$$

β_A is defined as the constant environmental factor depending on R_{STDA} value of RSSI values arriving from transmitter A. Similar RSSI values can be utilized at the same measurement location for transmitters B, C and D as in Fig.1. Finally, an average threshold standard deviation, T_{STD} is considered for all the transmitter WSNs given as

$$T_{STD} = \frac{1}{4}\left(R_{STDA} + R_{STDB} + R_{STDC} + R_{STDD}\right) \tag{4}$$

T_{STD} identifies the average environmental conditions due to the fact that RSSI values and the resultant R_{STD} values, change with respect to environmental conditions.

β_A is defined in terms of T_{STD} and R_{STDA} as

$$\beta_A = \frac{1}{2}\left(1 + \frac{T_{STD} - R_{STDA}}{T_{STD}}\right) \quad \text{for} \quad T_{STD} \ge R_{STDA} \tag{5}$$

$$\beta_A = \frac{1}{2}\left(1 - \frac{R_{STDA} - T_{STD}}{T_{STD}}\right) \quad \text{for} \quad T_{STD} < R_{STDA} \tag{6}$$

Calculated $RSSI_A$ value in equation (3) is considered as stable if $R_{STDA} \le T_{STD}$ and β_A is calculated as $\beta_A \in$ (0.5, 1). Calculated $RSSI_A$ value is considered as unstable if $R_{STDA} > T_{STD}$ and β_A is calculated as $\beta_A \in$ (0, 0.5).

Environmentally adaptive $RSSI_A$ value is calculated by substituting β_A , R_X and R_Y values in equation (3). Similarly, adaptive $RSSI_B$, $RSSI_C$, $RSSI_D$ values can be calculated at the same measurement point.

III. VIRTUAL FINGERPRINT GENERATION

In classical fingerprint map generation, RF signal amplitudes arriving from transmitter WSNs at each grid point are measured as the fingerprint at that point. Map of these points is termed as the fingerprint map. Hence, fingerprint map contains a collection of RF signal amplitudes corresponding to all the transmitters at each grid point. Signal amplitude measurements at object points are compared with the signal amplitude measurements at grid points of the fingerprint map. Closest grid points are used in position calculations.

Virtual fingerprint map, on the other hand, is generated by using theoretical RF signal amplitude distributions instead of physical measurements. Free space propagation of RF signals between a transmitter and a receiver is modeled for this purpose. Exponential signal amplitude decrease between a transmitter and a receiver against distance is formulated by equation (7) and plotted in Fig 2.

$$Y = C\, e^{-ax} \tag{7}$$

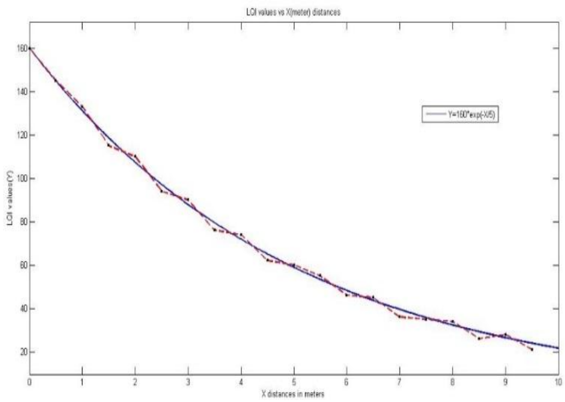

Figure2: RSSI distribution against distance between a transmitter and a receiver

RSSI amplitude, Y, is calculated by using equation (7) at every grid point with radiated signal strength C of a transmitter and x distance between the grid point and this transmitter. ‘a’ is the decay constant generated during measurements. Hence, virtual RSSI amplitudes at grid points are calculated by using radiated signal strengths of transmitters and the distances of grid points from these transmitters with equation (7). A 3D histogram map of calculated RSSI amplitudes at grid points for transmitter A is displayed in Fig. 3.

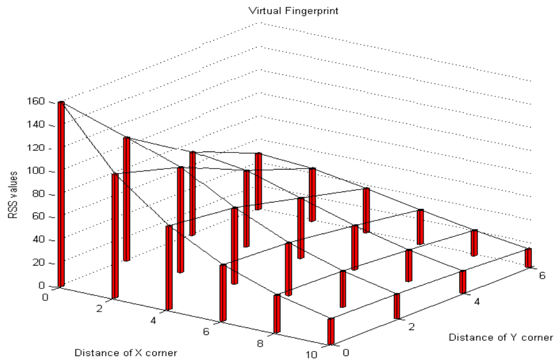

Figure3: Virtual fingerprint map across the test area for one transmitter

3D map in Fig.3 is termed as the virtual fingerprint map and it is generated for one radiated signal amplitude from a transmitter at an instant of time. Similarly, N number of virtual fingerprint maps can be generated from N number of signal amplitudes radiated from one transmitter. Hence, N numbers of virtual RSSI values can be obtained at each grid point from each transmitter.

RF signal transmission from transmitters displays random behavior in time domain and constant C in equation (7) randomly changes. This is also reflected in virtual RSSI amplitude calculations at every grid point. N number of virtual RSSI amplitudes are adaptively corrected and reduced to one virtual signal amplitude for one transmitter at each grid point. Final virtual fingerprint map consists of adaptively corrected virtual RSSI values as many as the number of transmitters at every grid point.

Similarly, N numbers of RSSI values are received by the object receiver from each transmitter. They are also adaptively corrected and their number is reduced to the number of transmitters. Localization algorithms are deployed with these final adaptively corrected virtual fingerprint map and final adaptively corrected object RSSI recordings to determine the object location.

IV. EXPERIMENTATION AND RESULTS

A rectangular area of 10mx6m with a grid spacing of 1m is employed for tests and measurements. It was a part of a sports hall with minimum obstacles. WSN transmitters are placed at the corners at a uniform height of 3 meters. A student with a WSN receiver is considered as the mobile unknown object. Jennic type WSN transmitters and receivers are deployed [13]. RF signals emitted from the transmitters are received by the object receiver and stored in a database in a server computer wirelessly interfaced to the receiver.

Initially, calibration experiments of the transmitted RF signals are conducted across the test area. Transmitted RF signal amplitudes are plotted against the distances between transmitters and receivers as shown in Fig. 2. This is repeated for all the transmitters and the object receiver. An average curve, RSSI amplitude versus distance, is generated to derive the equation (7).

a) Virtual Fingerprint map

At the end of the calibration stage, equation (7) is generated to calculate the virtual RSSI values at grid points. Grid distance to each transmitter is the x value in equation (7). 4 virtual RSSI amplitudes with respect to 4 transmitters are calculated at every grid point and a virtual fingerprint map is realized.

b) Localization

Adaptively corrected Virtual fingerprint map and object RSSI recordings for 4 transmitters are deployed and object location is calculated by using localization algorithms such as k-NN and weighted k-NN across the test area. In case of k-NN algorithm, 'k' number of nearest grid points to the unknown object location are selected by considering the smallest signal strength differences between the grid and object points identified as Euclidean distances. The object coordinates can be defined as the average values of these nearest grid coordinates. In case of weighted k-NN algorithm, the nearest grid points are individually weighted with respect to their Euclidean distances with the object. The object coordinates can be defined as the summation of the weighted coordinates.
Experimental results with physical and virtual fingerprint mapping are presented in Fig.4. Object locations are determined by using k-NN and weighted k-NN algorithms in both mapping techniques. No adaptive RSSI corrections are employed in this phase.

Secondly, N number of consecutive RF signal transmission from each transmitter is carried out and N number of virtual fingerprint map is generated for a single transmitter. This constitutes N number of virtual RSSI values at each grid point for each transmitter. Similarly, N number of RSSI recordings is also carried out at unknown object location.

Finally, N number of virtual RSSI recordings at each grid point and N number of object RSSI recordings for each transmitter are subjected to adaptive RSSI correction procedures. A resultant virtual fingerprint map is generated with 4 virtual adaptive RSSI values for 4 transmitters at each grid point together with 4 adaptive RSSI recordings for 4 transmitters at object point.

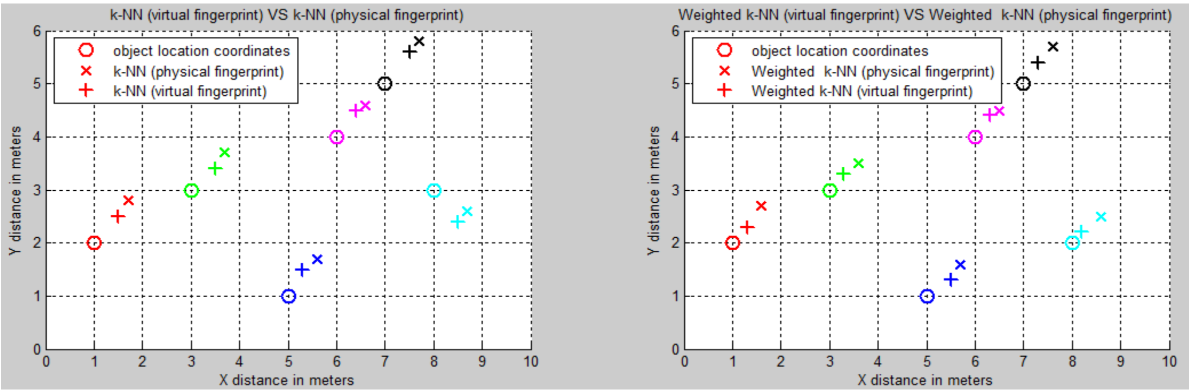

Figure 4: localization with virtual and physical fingerprinting with no adaptive correction

Actual object coordinates are compared with the calculated object coordinates. The results revealed an average error distance of 66cm with a grid space of 1m using virtual fingerprint map. Secondly, adaptively corrected virtual fingerprint map and adaptively corrected object RSSI recordings are deployed and object location is calculated by using k-NN and weighted k-NN algorithms. The results are presented in Fig. 5.

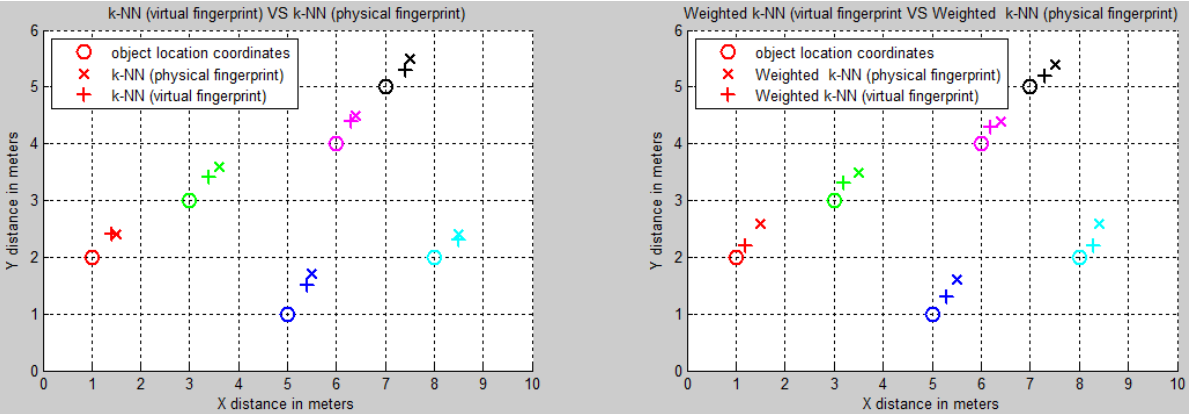

Figure 5: Localization with virtual and physical fingerprinting with adaptive correction

As it is seen in Figure 5, object localization accuracies are better with adaptively constructed virtual fingerprint map and adaptively corrected object RSSI recordings.

c) Results

In literature, Object localization accuracies calculated with physical fingerprint maps are generally around one grid space. This is also realized in current study. Average localization accuracy calculated with physical fingerprint map is found to be 96 cm with a grid space of 1m. On the other hand, average localization accuracy becomes 66cm with virtual fingerprint map employing the same grid space.

Adaptive RSSI corrections are applied on both physical and virtual fingerprint maps together with object RSSI recordings. As it is seen in Figure 5, the localization accuracies are quite improved compared to Figure 4. Weighted k-NN method with adaptively corrected virtual fingerprint maps and object RSSI recordings gives the minimum average localization error of 35cm with a 1m grid space.

V. CONCLUSIONS

A hybrid fingerprint localization technique is developed which is environmentally adaptive and deploys virtual fingerprint mapping. Previously, fingerprint maps are generated by making measurements at every grid point and these measured RSSI values are stored in a database. Unknown object RSSI recordings are later compared with the stored fingerprint values and location of the object point is estimated by averaging the nearest grid point coordinates.

In this study, RSSI values at grid points are calculated theoretically based on RSSI distributions in free space. Fingerprint map which is generated by these theoretical RSSI values is termed as virtual fingerprint map. This mapping technique saves a lot of time and effort in RSSI measurements and recordings. Initially, calibration curves between transmitters and receivers and their mathematical formulation are determined across the test area.

Once the virtual fingerprint map is established, RSSI values on the map and recorded RSSI values at object locations are adaptively adjusted to reduce the random variations among them. Two popular localization algorithms, k-NN and weighted k-NN, are used in these calculations. Best localization accuracies are obtained with weighted k-NN algorithm and adaptively corrected virtual fingerprint map.

Finally, it can be concluded that the important issue in this study is to prove the validity of virtual fingerprint mapping technique coupled with adaptive RSSI correction. The accuracy results prove that localization of objects can produce an accuracy of around 1/3 of the grid space. This is a good improvement among localization techniques without making too many RSSI measurements and including the effects of environmental problems.

REFERENCES

[1]. P.K. Singh, B. Tripathi, N.P. Singh, "Node localization in wireless sensor networks", International Journal of Computer Science and Information Technologies, Vol. 2 (6), 2011, pp 2568-2572

[2]. J. Kuriakose, S. Joshi, V.I. George, "Localization in Wireless Sensor Networks: A Survey", CSIR Sponsored X Control Instrumentation System Conference - CISCON-2013, pp 73-75

[3]. G. Chandrasekaran, M.A. Ergin, J. Yang, S. Liu, Y. Chen, M. Gruteser, R.P. Martin, "Empirical Evaluation of the Limits on Localization Using Signal Strength", 6th Annual IEEE Communications Society Conference on Sensor, Mesh and Ad Hoc Communications and Networks, 2009, pp 1-9

[4]. K. Almuzaini, A. Gulliver, "Range-Based Localization in Wireless Networks Using Density-Based Outlier Detection," Wireless Sensor Network, Vol. 2 No. 11, 2010, pp. 807-814
[5]. T. He, C. Huang, B.M. Blum, J.A. Stankovic, T. Abdelzaher, “Range-Free Localization Schemes for Large Scale Sensor Networks”, Proceedings of the 9th annual international conference on Mobile computing and networking, 2003, pp 81-95
[6]. V. Kunin, M. Turqueti, J. Saniie and E. Oruklu, "Direction of Arrival Estimation and Localization Using Acoustic Sensor Arrays", Journal of Sensor Technology, Vol. 1 No. 3, 2011, pp. 71-80
[7]. Zhang, R., Guang, J., Chu, F.H., Zhang, Y.C.: ‘Environmental adaptive indoor radio path loss model for wireless sensor Networks localization’,Int. J. Electron. Commun., 2011, 65, pp. 1023–1031
[8]. Larranaga, J., Muguira, L., Manuel, J., Vazquez, J.: ‘An Environment Adaptive ZigBee based Indoor positioning Algorithm’. Int. Conf, on indoor Positioning and Indoor Navigation (IPIN), Zurich, 2010,pp. 15–17
[9]. J. Larranaga, L. Muguira, J.M.L. Garde, J.I. Vazquez, “An environment adaptive ZigBee-based indoor positioning algorithm”, International Conference on Indoor Positioning and Indoor Navigation (IPIN), 2010, pp 1-8
[10]. H. Koyuncu, S.H.Yang, “Indoor Positioning with Virtual Fingerprint Mapping by Using Linear and Exponential Taper Functions”, IEEE International Conference on Systems, Man, and Cybernetics 2013, pp 1052 – 1057
[11]. Wendell T.Hill ,Electromagnetic radiation Wiley , 2009 , ISBN 978-3-527-40773-6.
[12]. T.S.Rappport. Wireless Communications: principles and practise , Prentice-Hall Inc.,New Jersey ,1996
[13]. http://www.jennic.com/jennic_support/application_notes/jnan-1052_home_sensor_demonstration